

Chapter 4

Characterisation of a Polymeric Multilayer Model

4.1 Introduction

Polymer multilayers are used in a variety of industries such as patches for drug delivery or laminates used to protect food, while retaining aroma and flavours to extend shelf life^{1, 2}. The quality, integrity and spatial/lateral composition of such films are vital to ensuring optimal function. ToF-SIMS has been shown to be a suitable technique for understanding the distribution of components through thickness due to its high chemical sensitivity^{3, 4}. In this chapter model multilayer films are produced composed of the fully characterised codeine/PLA blends described in depth in Chapter 3 and the water soluble film forming polymer hydroxypropyl methylcellulose (HPMC). Through analysis of this multilayer model using pharmaceutically relevant drug delivery polymers, the potential capabilities of the ToF-SIMS for the study of real world multilayers can be explored.

HPMC is a non-ionic water-soluble cellulose ether which is commonly used in oral controlled-release preparations⁵⁻⁹ and for film coatings¹⁰. HPMC is soluble in water but not chloroform, spin casting codeine/ PLA layers from chloroform on top of the HPMC is used to allow for layer separation. This reduces the occurrence of mixing of the layers. HPMC has not previously been depth profiled and as such this system illustrates the sputtering performance of HPMC. The bio-polymer polycaprolactone (PCL) has been successfully depth profiled and is the closest chemically to HPMC previously investigated. However PCL showed evidence of ion induced damage production¹¹ that may influence this analysis.

The analysis of polymeric multilayer films provides a considerable challenge owing to the variability in sputter characteristics found between different polymers under sputtering. Polymers can be differentiated into type I and type II polymers. Type I, including HPMC, which typically cross link when sputtered, often have aromatic groups and limited branching. This introduces weak points

susceptible to damage under sputtering¹². Type II polymers typically degrade under sputtering through random chain scission. As indicated by the results of Chapter 3, PLA is such a polymer. A specifically challenging formulation for depth profiling has been used in this work to determine whether ToF-SIMS is capable of sputtering multilayers with different properties and still provide meaningful chemical characterisation. The rationale behind this is due to the range of polymers used in industry for the production of such films, building on confidence gained from the initial work set out in Chapter 3.

The work in this chapter aims to produce a model multilayer therapeutic formulation and to analyse it with ToF-SIMS depth profiling. The rationale behind this is to study whether the technique is capable of scrutinising drug distribution in systematically produced bilayer and trilayer multilayer films, with a range of polymer/polymer and polymer/silicon interfaces.

4.2 Experimental

4.2.1 Polymer Solution Production

A 10 mg/ml solution of a 28.6% (w/w) blend of codeine (Sigma Aldrich) and PLA (Polysciences, Warrington, PA) was used in this work as described in Chapter 3. Piranha etched and cleaned silicon wafers measuring 1 cm² were cut and cleaned for spin casting, all fully described in Chapter 3 of this thesis. HPMC (viscosity 4,000 cP, for a 2% (w/v) H₂O solution, Sigma Aldrich, Dorset, UK) was dissolved in ultrapure water to produce a 1% (w/v) solution. Half of the water was heated to 85°C before the addition of HPMC and the remaining half (at room temperature) was added. The solution was then placed in the fridge overnight to allow the HPMC to dissolve completely. This process was undertaken as HPMC will congeal into an amorphous gel and not dissolve if placed in cold water however in warm water it will homogeneously distribute within the solvent which is then quickly cooled. A 1% (w/v) solution was produced as this provides sufficient viscosity allowing for spin casting to be undertaken but is not so concentrated that it could not be easily drawn into a pipette. HPMC was prepared the day before spin casting and stored in a fridge overnight in order to reduce

possible contamination. Multilayers were produced shown in the schematic below (Figure 4.1).



Figure 4.1 Schematic representation of the a) bilayers and b) trilayer films produced in this study with red layers indicating PLA/codeine film, green layers indicate HPMC film and the silver layer represents the piranha solution cleaned silicon substrate.

4.2.2 Ellipsometry

Ellipsometry was undertaken 15 min after each stage of solution deposition in an attempt to determine the thickness of each layer within the film and to provide an understanding of whether there is spin casting induced roughening caused by casting polymer layers on top of substrate films. An alpha-SE spectroscopic ellipsometer (J. A. Woollam Co., Inc., Lincoln, NE) was used to determine film thickness. As in Chapter 3, piranha cleaned silicon wafers were analysed in triplicate to determine the average SiO₂ layer thickness of 1.74 ± 0.05 nm which was subtracted from the thickness measured of the bottom layer.

4.2.3 ToF-SIMS and Depth Profiling

The same instrument, software and experimental conditions used in Chapter 3 for ToF-SIMS depth profiling were used for all depth profiling of these films.

4.3 Results and Discussion

Multilayer films were produced and analysed with ToF-SIMS depth profiling and ellipsometry in order to determine the capabilities of ToF-SIMS to show the distribution of constituents through thickness of a multilayer drug delivery model. As described previously in Chapter 3, the selection of ions is important for depth profiling. The $C_2H_6N^+$ (m/z 44) cation was used to monitor the codeine distribution, due to higher intensity than the molecular ion. The $C_3H_7O^+$ (m/z 59) ion corresponds to the intact hydroxypropyl sidechain on the HPMC molecule and was selected to monitor HPMC as this not prominent in the spectra for either PLA or codeine. Unlike in Chapter 3, the $C_3H_4O^+$ radical cation at m/z 56 was used as diagnostic for PLA as the $C_3H_3O^+$ ion at m/z 55 is an ion common to both PLA and HPMC.

4.3.1 Bilayer Systems

Figure 4.2a shows the ToF-SIMS depth profiling data from a bilayer containing a codeine/PLA layer spun cast on top of a HPMC layer, supported on a silicon substrate. Figure 4.2b shows the ion image data in the XZ viewing plane for all ions plotted in Figure 4.2a with an additional overlay of the codeine, PLA and HPMC ion intensities with interface positions labelled. Figure 4.2c displays an XY cross section of the characteristic ions of codeine, PLA and HPMC within each respective layer. This measurement was taken near the interfaces at the instant the steady-state was reached. For all subsequent figures in this chapter the organisation of the figure is maintained as described here.

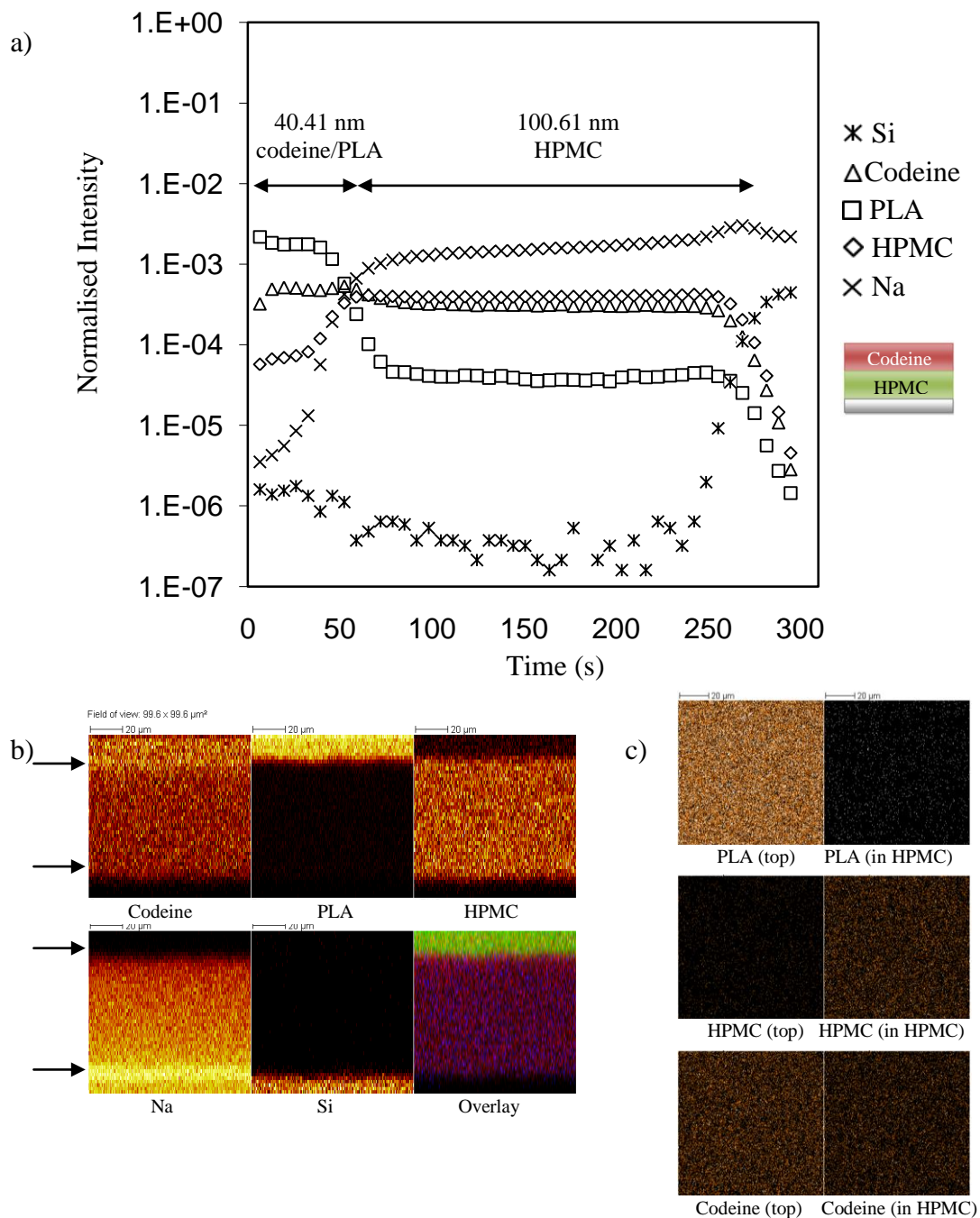


Figure 4.2 a) ToF-SIMS depth profile showing ions of significance for a bilayer film of codeine/PLA cast on top of a HPMC film onto a silicon wafer. The contaminant sodium is also displayed and values indicate ellipsometrically derived layer thickness. b) Ion images taken from the XZ axis with interfaces marked by arrows, the overlay shows codeine (red), PLA (green) and HPMC (blue). c) Ion images taken in the XY axis for two adjacent scans summed from the top layer and the bottom layer.

In Figure 4.2a the presence of a thin codeine/PLA layer is observed at the top surface that is sputtered through after 48 s. The same method to determine the interface as described in Chapter 3^{13, 14} at the location of the half maximum of the silicon ion intensity (m/z 28) was used. For the polymer-polymer interface shown in Figure 4.2a the half maximum of the HPMC (m/z 59) intensity was used, for subsequent figures either PLA or HPMC was used depending on which was the substrate film. With knowledge of the duration of sputtering and film thickness, the sputter rate for each film can be determined assuming uniform sputtering. This will be discussed further in this section.

Looking first at the top layer of the bilayer systems in Figure 4.2a, PLA is at a greater intensity at the outer interface than codeine, which is depleted at the surface. The codeine intensity immediately increases to a steady state with a corresponding decline in PLA ion intensity after sputtering for a few seconds as found in the single layer model shown in Chapter 3. The plot in Figure 4.2a indicates a low intensity (at least an order of magnitude less than codeine or PLA) of the HPMC indicating ion is present at the outermost surface. This intensity gradually increases through the depth of the codeine/PLA layer towards the interface with the HPMC film. This indicates the presence of low intensity m/z 59 ions in the codeine/PLA layer near the interface with the underlying HPMC layer. As the HPMC ion intensity increases there is a concurrent decline in PLA and codeine intensity. However it is noted there appears to be a slight increase in codeine ion intensity at the polymer-polymer interface, similar to that found in Chapter 3 at the silicon interface which was more prominent in lower codeine loadings. It is also noted that the decline in codeine ion intensity does not appear to be as significant as that observed for PLA, shown clearly in Figure 4.2b. With an increase in the 59 m/z ion intensity, there is also a dramatic increase in the sodium contaminant concentration, mirrored in Figures 4.2a and b, which maintains a steady state throughout the HPMC layer but shows enrichment at the silicon interface where the HPMC signal declines. Figure 4.2c indicates within each of the polymer layers there is a uniform distribution of characteristic ions across the area rastered. The majority of the secondary ions evoked from the polymers are localised within their respective layers however codeine displays a consistent secondary ion signal within the HPMC layer as well as within the codeine/PLA layer.

Figure 4.2a suggests a sputter rate of 0.84 nm s^{-1} for the codeine/PLA layer which is similar to the 0.79 nm s^{-1} recorded in Chapter 3. HPMC appears to sputter at a slower rate of 0.44 nm s^{-1} . The disparity between the sputtering rates determined causes the plotting of depth on the x-axis less reliable and indicates matrix effects may influence the analysis of these multilayer films. The presence of HPMC indicating ions in the top codeine/PLA film may be due to the presence of low intensity m/z 59 signals in the PLA and/or codeine spectra or to sputter induced surface roughening¹⁵. This is where uneven topography is generated through variable sputter rates across the sputter raster area, causing one part of the codeine/PLA film to be degraded at a faster rate, exposing the underlying HPMC marginally earlier in a flat film model. Alternatively uneven topography at the outermost surface or at the polymer-polymer interface could also cause a gradual increase in intensity by acting as a template for the remaining depth profile. However both of these scenarios would be expected to show a parallel decline in PLA intensity. The ion images in Figure 4.2c however indicate that uneven topography or variability in sputter rate across the area analysed is unlikely to be responsible for this as the increase in HPMC is found to be laterally consistent across the interface. Whilst HPMC is insoluble in chloroform, some intermixing may have occurred at the polymer-polymer interface with the organic solvent causing swelling of the HPMC layer. The sodium enrichment at the silicon interface suggests preferential segregation to this interface. As sodium is easily ionisable, on encountering the significantly more resilient silicon wafer, ion impacts can cause greater secondary ion emission which may exaggerate the degree of enrichment¹⁶.

The m/z 44 secondary ion intensity used to follow codeine is found to decline on entering the HPMC layer, however it is proportionally less than the drop in PLA concentration which is also observed for the codeine molecular ion at m/z 300 (not shown). As codeine is soluble in water as well as chloroform, diffusion of chloroform into the underlying HPMC layer may have lead to codeine diffusing into the HPMC substrate which has been clearly resolved by ToF-SIMS molecular depth profiling. The high molecular weight of the PLA may have restricted the penetration into the HPMC polymeric matrix in contrast to the relatively lower molecular weight of codeine, which may be able to diffuse through the entangled polymer network of the chloroform swollen HPMC interface. The data presented

here shows the sensitivity of ToF-SIMS to determine the distribution of chemical components through thickness, presenting the ability to detect the transport of the drug from one polymer layer into another during manufacture. By reversing the multilayer composition inferences can be made as to the mechanism of component distribution, as shown in Figure 4.3.

By altering the order in which the layers are deposited, the interface between the two layers in the depth profile (with the same scale on the x-axis as that in Figure 4.2a) was shown to be altered significantly. When depositing a HPMC layer on a codeine/PLA polymer substrate, the surface transient region appears to have minimal effect on the intensity of the HPMC signal intensity compared to that observed with PLA in Figure 4.2a at the outer film surface. Throughout the top HPMC layer, the m/z 59 signal indicative of HPMC remains constant and the ions associated with codeine and PLA intensity remains at an order of magnitude lower in intensity at a steady state. The sodium ion intensity is found to be depleted in the outermost surface of the film. However it increases to reach a steady state within the bulk of the HPMC layer. A far broader interface between the two polymer layers with this layer configuration is observed than shown in Figure 4.2a. PLA and codeine intensity is seen to gradually increase and codeine ion intensity is observed to become more intense than the PLA in the codeine/PLA layer. The intensity of codeine, PLA and sodium are seen to remain intense, although declining after reaching the maximum of the silicon intensity. This illustrates the broadening of the interfaces by suggesting incomplete sputter removal of the polymer layers on reaching the silicon substrate.

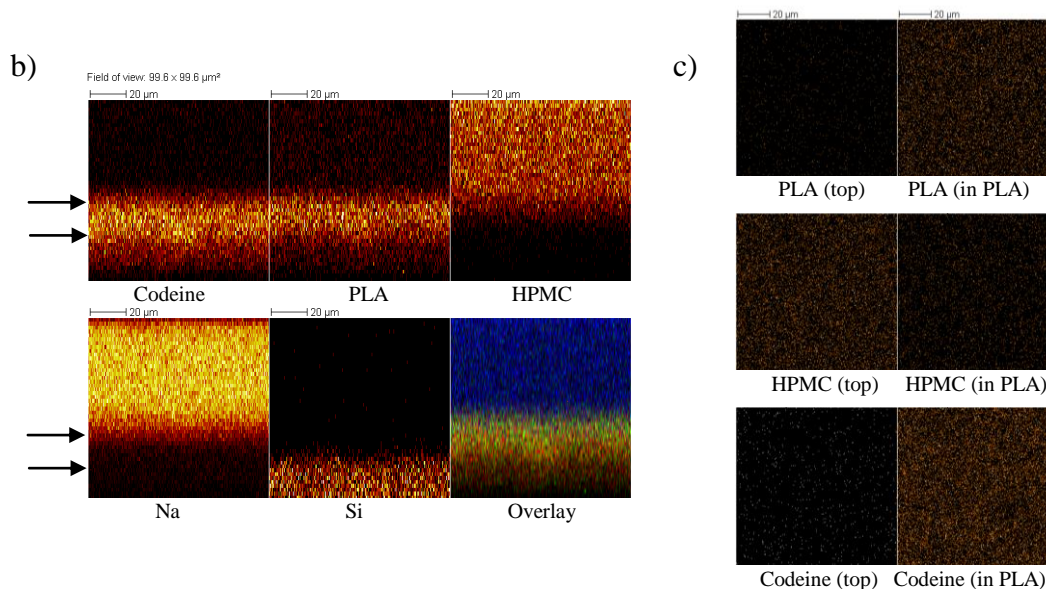
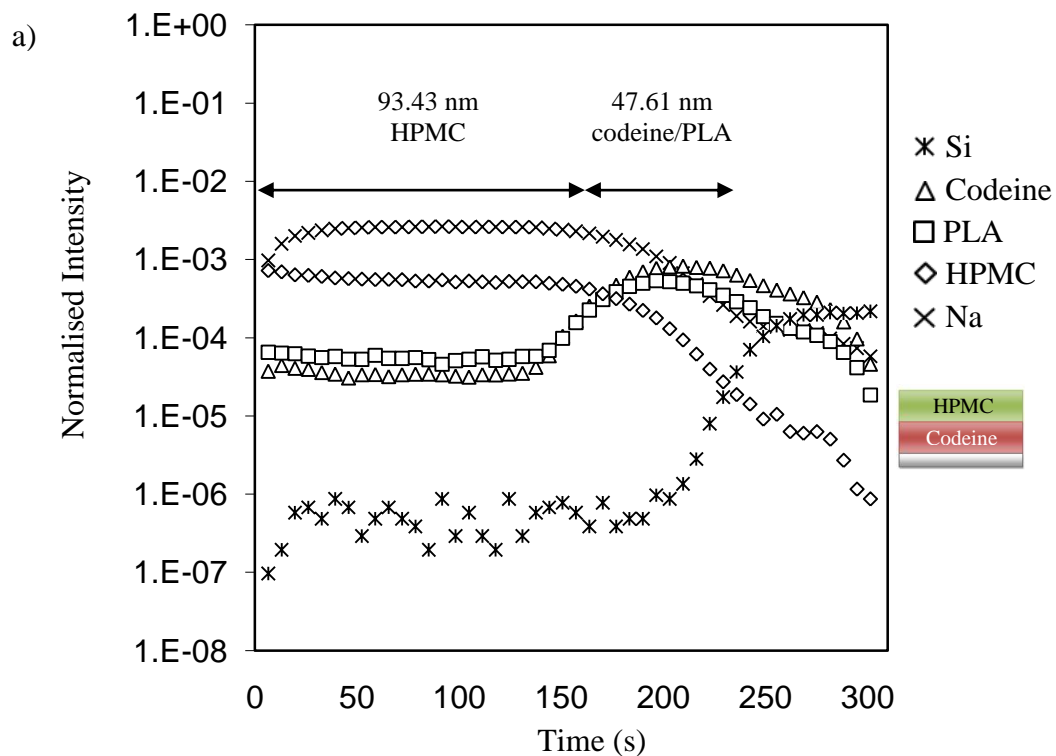


Figure 4.3 a) ToF-SIMS depth profile showing ions of significance for a multilayer film where HPMC is cast onto a codeine/PLA film cast on a piranha solution cleaned silicon wafer. The contaminant sodium is also displayed and values indicate ellipsometrically derived layer thickness. b) Ion images taken from the XZ axis with interfaces marked by arrows, the overlay shows codeine (red), PLA (green) and HPMC (blue). c) Ion images taken in the XY axis for two adjacent scans summed from the top layer and the bottom layer.

Importantly Figures 4.3b and c suggest codeine has not diffused into the HPMC layer above it, (during the exposure to the water solvent used for HPMC.) This is seen as the low intensity of codeine in the top layer of Figure 4.3c suggesting the mechanism through which codeine is distributed in Figure 4.2 occurs during the spin casting procedure from chloroform on top of the HPMC layer. This observation will be further investigated with trilayer models in section 4.3.2.

The great increase in interface width observed suggests an ion-beam induced damage mechanism³ for this observation, most influenced by the HPMC layer. When sputtering through the HPMC with its slower rate of sputtering and thus lower sputter yields, this model suggests an accumulation of damaged molecular fragments are produced¹¹. This is a matrix effect most prevalent when sputtering through HPMC cast on a PLA substrate, which itself has greater sputtering yields. HPMC is prone to cross linking which has been shown to fare worse in molecular depth profiling than those less prone like PLA^{17, 18}. Ion-induced damage is caused where the balance between secondary ion generation and sputter removal of damage is less than favourable^{3, 19}.

The bismuth primary ion dose in a dual beam experiment is also influential in rationalising the interface widths observed²⁰. High energy bismuth ions are capable of generating sufficient molecular damage/rearrangement so as to make C_{60}^+ sputtering inefficient at removing the damage done by the analysis beam and hence broadening interfaces. As a result of the matrix effect highlighted in the last two paragraphs, broadening of interface widths and intermixing at the polymer-polymer interface may occur when HPMC is cast on a polymer substrate, but not necessarily in the opposite conformation. Within the codeine/PLA layer, codeine reaches a greater intensity than that found for the PLA indicating ion, which is complimentary to the data shown in Chapter 3. By creating trilayers the sputtering behaviour of these multilayers can be assessed shown in section 4.3.2.

The bilayers presented indicate the mechanism through which codeine enters the HPMC layer is likely to be an effect of the chemistry and mechanism of film production as opposed to matrix effects described. Chloroform is a highly volatile solvent and is able to penetrate through percolation and swelling of non-solvent films such as HPMC. A possible mechanism for the observation of higher

intensity codeine signals in a substrate HPMC layer when casting PLA drug layer on top than when the layer order is reversed is HPMC swelling on addition of chloroform. This acts to draw in the small mobile codeine molecules (m/z 299) through diffusion, whereas the larger PLA chains (55 kDa) are unable to be drawn into this HPMC substrate. Once the remaining chloroform has evaporated from within the model system, the codeine remains entrapped within the collapsed polymer chains of the HPMC layer underneath²¹. This demonstrates how ToF-SIMS can help provide a novel method for understanding the distribution of small molecule drugs within the structure for use in multilayer film drug delivery applications. It also highlights a limitation of the technique with respects to the broad interfaces and variation in sputter rates for different materials.

4.3.2 Trilayer Systems

Creating alternating trilayers was then used to determine whether ToF-SIMS is capable of characterising constituent distribution where multiple polymer interfaces are involved shown for a HPMC-codeine/PLA-HPMC multilayer in Figure 4.4 below.

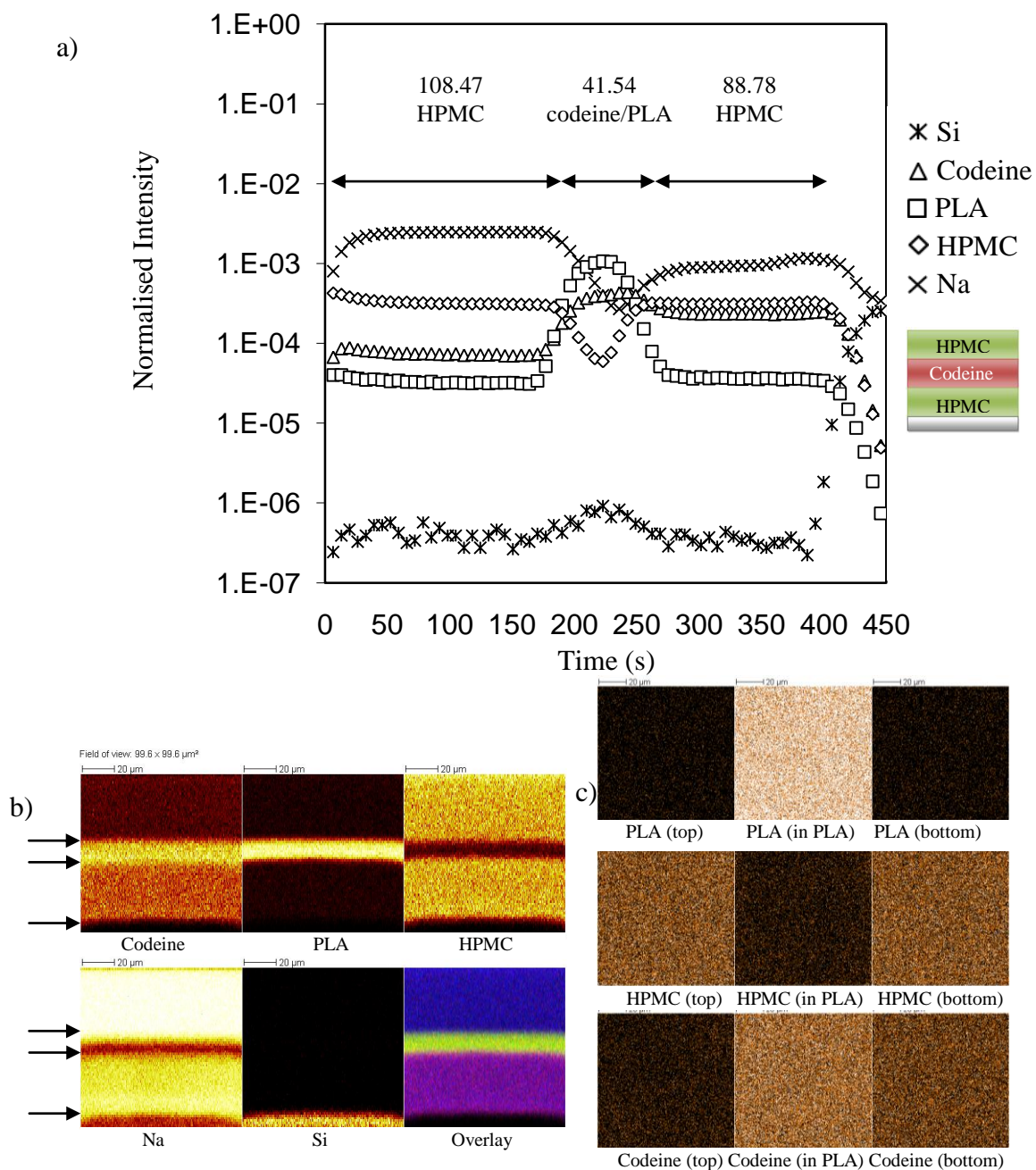


Figure 4.4 a) ToF-SIMS depth profile showing ions of a multilayer film with alternating layers of HPMC above and below a codeine/PLA film, all three layers are cast on top of a piranha solution cleaned silicon wafer. The contaminant sodium is also displayed and values indicate ellipsometrically derived layer thickness. b) Ion images taken from the XZ axis with interfaces marked by arrows, the overlay shows codeine (red), PLA (green) and HPMC (blue). c) Ion images taken in the XY axis for two adjacent scans summed from the top, middle and the bottom layers. Explanation for the increased secondary ion counts can be found in Appendix 1.

The top HPMC layer at the air-polymer interface shown in Figure 4.4a appears to have a similar profile to that shown in Figure 4.3a. However the m/z 44 ion used to track codeine begins initially at a higher secondary ion intensity to the PLA fragment ion. On encountering the interface of HPMC with codeine/PLA, there is a concomitant rise in the signals for PLA and codeine with a drop in the signal for the HPMC film. There is a noticeable lag in the decline of the sodium signal, suggesting some sodium penetration into the middle codeine/PLA layer. In the middle codeine/PLA layer, PLA is found to symmetrically increase in intensity then decline on approaching the underlying HPMC substrate film. The HPMC signals increase at this interface, showing a symmetrical change in signals through the three films. Similar observation may be made for the PLA signals across the interfaces. In contrast, the behaviour of the signal for codeine does not follow this pattern. The m/z 44 ion increases in intensity along with the PLA ion at the interface between the top HPMC layer and the PLA/codeine film. It is seen to reach a plateau value and rather than decreasing as the interface with the underlying HPMC approaches. There is a slight increase in the codeine intensity suggesting enrichment at the interface. The codeine signal is then seen to decline marginally and does not return to the level seen in the top HPMC layer as observed with PLA, which was indicated by the depth profile in Figure 4.2. This is clearly exhibited in the overlay shown in Figure 4.4b and the XY cross sections from within individual polymer layers shown in Figure 4.4c.

The steady state sodium signal is found to have declined in the second HPMC layer compared with that observed in the top layer which may be due to the increase in the secondary ion yield of m/z 44 ions. A strong enrichment at the silicon interface similar to that seen in Figure 4.2 is observed indicating that when casting HPMC on a silicon substrate the sodium segregates to the substrate interface. When casting onto a polymer film substrate, sodium instead will penetrate the layer below, suggesting a preferential distribution of sodium to the substrate interface when spin casting.

The data presented here appears to further support the mechanism that spin casting from chloroform on top of a HPMC layer causes a swelling of the HPMC layer. This increases the solubility to codeine, shown as remaining intense in the bottom HPMC layer. The reversion of PLA and HPMC back to the intensities

observed in the top HPMC layer is another strong indication that the presence of codeine in the HPMC is not an instrumentation affect but in fact due to drug migration.

The interfaces between the two HPMC layers and the codeine/PLA layer between them appear to be symmetrical when monitoring the characteristic ions for PLA and HPMC. As such any significant ion beam induced damage cannot be observed in this trilayer film as would be expected the bottom interface would be far sharper than the top interface. This is due to faster, more uniform depth profiling through the more easily sputtered PLA layer. While the bottom interface is marginally sharper (~3 seconds less sputtering required to reach the bottom interface using an 84:16 regime³) this is not significant enough to draw conclusions from.

In comparison with Figure 4.3, the interface width of the top interface of Figure 4.4 is improved by ~13 s. This suggests beam induced mixing is not a consistent phenomena as its effects are lower at the top polymer interface of the trilayer than in the equivalent bilayer model shown in Figure 4.3. Further support for this is shown in Figure's 4.3b and c and 4.4b and c whereby in the bilayer the HPMC appears less homogeneous in the PLA layer. This indicates roughening (as shown by more void spaces in secondary ion yield, in addition to greater overlapping of secondary ion signals between PLA and HPMC), more than in the trilayer. Reversing the alternating multilayers to comprise two codeine/PLA layers separated by the middle HPMC layer was the final configuration investigated shown in Figure 4.5.

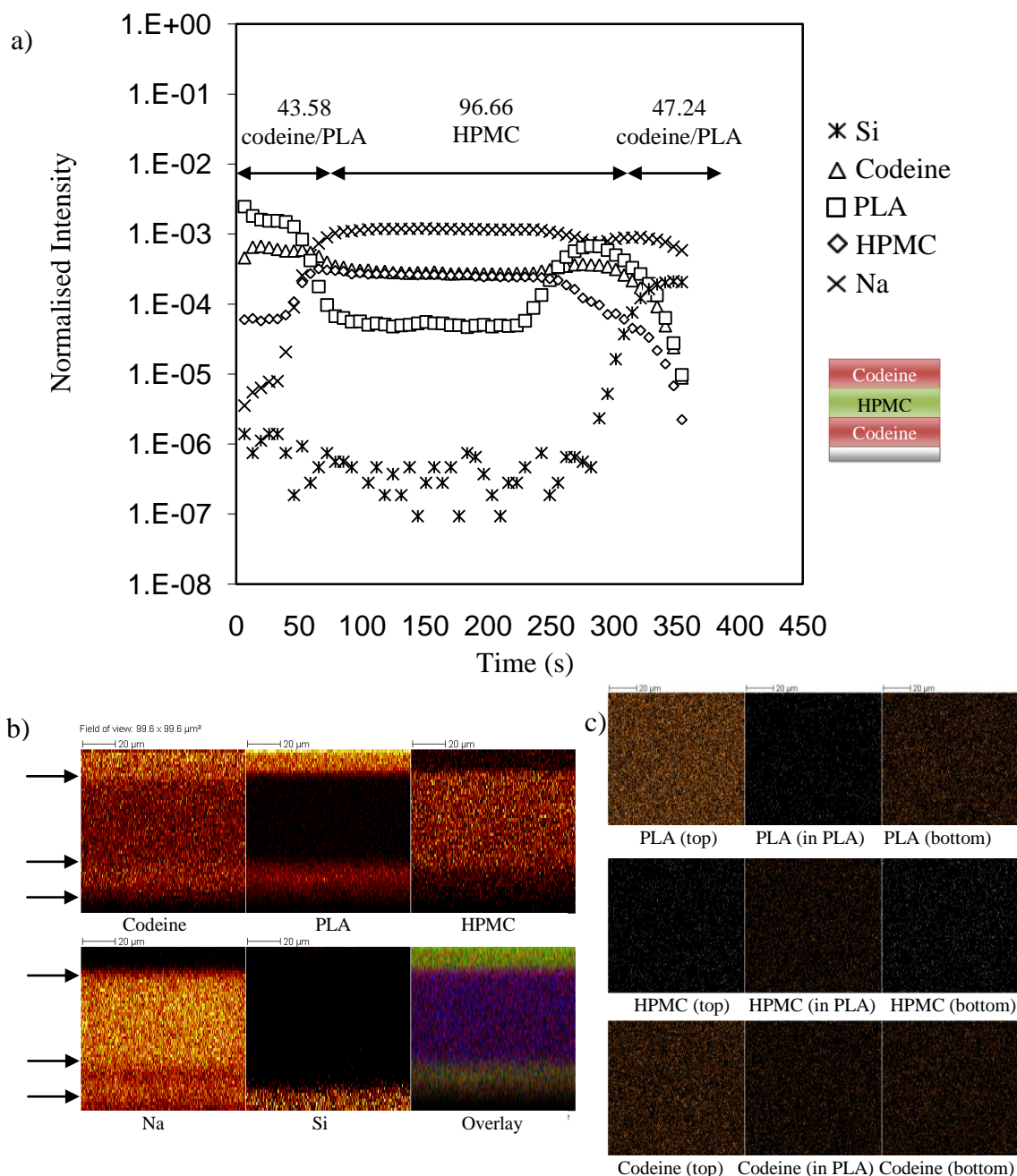


Figure 4.5 a) ToF-SIMS depth profile showing ions of a multilayer film with alternating layers of codeine/PLA above and below a HPMC film, all three layers are cast on top of a piranha solution cleaned silicon wafer. The contaminant sodium is also displayed and values indicate ellipsometrically derived layer thickness. b) Ion images taken from the XZ axis with interfaces marked by arrows, the overlay shows codeine (red), PLA (green) and HPMC (blue). c) Ion images taken in the XY axis for two adjacent scans summed from the top, middle and the bottom layers.

The depth profile shown in Figure 4.5a is remarkably consistent with the data shown in Figures 4.2 and 4.3 that indicates the casting of the outermost codeine/PLA layer on top of two polymer layers has not affected the films roughness and uniformity. Again, an enrichment of PLA is seen at the outer surface with a complementary reduction in codeine signal, overcome within a few seconds of sputtering. The only difference in the secondary ion characteristics in Figure 4.5a compared to those shown in Figures 4.2a and 4.3a is in the bottom codeine/PLA film codeine does not reach a greater intensity than the characteristic ion for PLA. Interestingly the codeine is shown to be uniformly distributed throughout the HPMC layer (as observed in Figure 4.2a) suggesting chloroform has penetrated throughout the HPMC layer, yet PLA and codeine are soluble in chloroform and as such the bottom layer may have been exposed to chloroform. As at least half an hour had passed between casting of the top and bottom layer the exposure to chloroform which had penetrated the middle HPMC layer may have been insufficient to cause significant damage to the bottom codeine/PLA interface (roughening). However it may have acted to draw some codeine into the HPMC layer above it which would explain the reduction in codeine intensity in the final layer, when compared with the results of Figure 4.3a. This justification however assumes matrix effects that could affect codeine intensity are not exacerbated by casting of an additional layer. Surface roughness and sputtering characteristics would also be similar to the data shown in Figures 4.2 and 4.3 as the interfaces between the two layers occur over a comparable range. While it is acknowledged that secondary ion generation over depth is an issue with depth profiling with C_{60}^{+22} , the ellipsometric data indicates these films are no thicker than 240 nm and as such these effects should be minimal. The secondary ion yield remains at a similar ratio (between PLA and HPMC) as that seen in Figure 4.3, supporting the damage model thought to be responsible for the observation of interfacial broadening.

The repeatability of ToF-SIMS depth profiling has been shown to be consistent over a number of days²³. As such the sputter rate for the codeine/PLA layer was expected to be similar to that observed in Chapter 3 with a C_{60}^{+} current of 200 pA which was observed. The average sputtering rate of codeine/PLA is calculated as being $0.78 \pm 0.11 \text{ nm s}^{-1}$ and for HPMC the rate is slower at $0.50 \pm 0.05 \text{ nm s}^{-1}$. The values quoted for the mean and standard deviation indicate a consistent and

reproducible sputter rate for the two polymer films regardless of a change in the substrate that films are deposited. For codeine/PLA the standard deviation is skewed by data shown in Figure 4.3 that indicated a sputter rate of 0.60 nm s^{-1} . This may be due to a limitation of the interface identification procedure, ion-beam induced damage or considerable intermixing reducing the sputter rate at that particular interface. It is noted for the bottom HPMC-codeine/PLA interface in Figure 4.5 the sputter rate was higher at 0.72 nm s^{-1} however this is still less than that observed for codeine atop HPMC. The inconsistency of the change in sputter rate between the 0.60 and 0.72 nm s^{-1} further supports a non-linear ion-beam induced damage/intermixing mechanism, which may be responsible for a reduction in sputter rate, which is only observed when HPMC is cast on top the codeine/PLA layer. The HPMC film is where the accumulation of damage takes place, which supports the literature which suggests sputtering of PLA yields reliable results up to $1 \mu\text{m}$ depths¹⁴. In addition, polymers which are susceptible to cross-linking fare worse under sputtering^{17, 24, 25} than those that degrade by depolymerisation²⁶ such as HPMC and PLA respectively.

4.4 Conclusions

ToF-SIMS has been shown to be able to describe for the first time the release of drug from a drug containing layer into an adjacent drug free polymer layer. This indicates how an understanding of the chemistry and the method of casting multilayer polymer films is vital for production of a therapeutically beneficial formulation. The characterisation of drug distribution through thickness of a challenging multilayer model has not previously been shown with ToF-SIMS, however owing to its high depth resolution and surface sensitivity it has proved capable of providing chemical information which can be related to the production process. Equipped with this knowledge, improved formulations can be produced for *in vivo* applications with greater efficiency. ToF-SIMS has been shown to be a useful analytical technique which is capable of highly consistent and repeatable depth profiling performance. HPMC has been found to be amenable to depth profiling with C_{60} , however it suffers from issues which affect polymers more prone to cross linking^{25, 27}, namely ion induced damage/mixing between layers³.

The literature has reported a reduction in the sputter rate at interfaces between polymer films due to ion-induced damage in the layer above, either generating roughness or contributing to intermixing³. This is considered more significant with type I polymers¹². Accurate molecular depth profiling requires the damage dealt to the surface when depth profiling to be removed by the ion impacts which caused it. With the advent of cluster ion sources for analysis and large polyatomic sputter sources such as C_{60}^+ the surface and bulk analysis capabilities of modern ToF-SIMS of organic materials have greatly improved. However there are still further improvements to be made in order to be able to depth profile in a manner that will maintain sharp interfaces between layers whilst keeping damage low, providing high depth resolution and maintaining secondary ion counts. Recent advances in the next generation of sputter sources, i.e. large argon cluster ions are showing great promise to be able to deliver such improvements²⁸. However recent work has suggested grazing angles of incidence of the ions and sample rotation are also valid methods to reduce broadening of the interfaces shown^{4, 23}.

The presence of codeine found within the HPMC layer when spun cast on top of this film, and the comparative low intensity of codeine ions found in the HPMC when the layer order was reversed, vitally shows the high depth resolution attainable with ToF-SIMS depth profiling of organic materials. This has not previously been shown for drug loaded multilayer films. This model may have been improved through using a 20 mg/ml solution of the 28.6% codeine/PLA film as film thickness would have been expected to be comparable. It is unknown if the relative film thicknesses may have affected factors such as the interface width. This capability of the SIMS technique in conjunction with the exciting current advances in primary ion and sputter sources suggest a promising future for the use of ToF-SIMS molecular depth profiling as a technique for characterising organic controlled release formulations, in order to rationalise their performance.

4.5 References

1. Bilbao-Sáinz, C., R.J. Avena-Bustillos, D.F. Wood, T.G. Williams, and T.H. McHugh, *Journal of Agricultural and Food Chemistry*, 2010. **58**(6): p. 3753-3760.
2. Kamper, S.L. and O. Fennema, *Journal of Food Science*, 1984. **49**(6): p. 1478-&.
3. Wagner, M.S., *Analytical Chemistry*, 2004. **77**(3): p. 911-922.
4. Sjovall, P., D. Rading, S. Ray, L. Yang, and A.G. Shard, *Journal of Physical Chemistry B*, 2010. **114**(2): p. 769-774.
5. Ishikawa, T., Y. Watanabe, K. Takayama, H. Endo, and M. Matsumoto, *International Journal of Pharmaceutics*, 2000. **202**(1-2): p. 173-178.
6. Siepmann, J., H. Kranz, R. Bodmeier, and N.A. Peppas, *Pharmaceutical Research*, 1999. **16**(11): p. 1748-1756.
7. Siepmann, J. and N.A. Peppas, *Advanced Drug Delivery Reviews*, 2001. **48**(2-3): p. 139-157.
8. Tahara, K., K. Yamamoto, and T. Nishihata, *Journal of Controlled Release*, 1995. **35**(1): p. 59-66.
9. Velasco, M.V., J.L. Ford, P. Rowe, and A.R. Rajabi-Siahboomi, *Journal of Controlled Release*, 1999. **57**(1): p. 75-85.
10. Sakata, Y., S. Shiraishi, and M. Otsuka, *International Journal of Pharmaceutics*, 2006. **317**(2): p. 120-126.
11. Fletcher, J.S., X.A. Conlan, N.P. Lockyer, and J.C. Vickerman, *Applied Surface Science*, 2006. **252**(19): p. 6513-6516.
12. Mahoney, C.M., *Mass Spectrometry Reviews*, 2010. **29**(2): p. 247-293.
13. Rafati, A., M.C. Davies, A.G. Shard, S. Hutton, G. Mishra, and M.R. Alexander, *Journal of Controlled Release*, 2009. **138**(1): p. 40-44.
14. Shard, A.G., P.J. Brewer, F.M. Green, and I.S. Gilmore, *Surface and Interface Analysis*, 2007. **39**(4): p. 294-298.
15. Shard, A.G., F.M. Green, P.J. Brewer, M.P. Seah, and I.S. Gilmore, *Journal of Physical Chemistry B*, 2008. **112**(9): p. 2596-2605.
16. Green, F.M., I.S. Gilmore, and M.P. Seah, *Rapid Communications in Mass Spectrometry*, 2008. **22**(24): p. 4178-4182.
17. Wagner, M.S., *Surface and Interface Analysis*, 2005. **37**(1): p. 42-52.
18. Pekel, N., F. Yoshii, T. Kume, and O. Güven, *Carbohydrate Polymers*, 2004. **55**(2): p. 139-147.
19. Gillen, G., D.S. Simons, and P. Williams, *Analytical Chemistry*, 1990. **62**(19): p. 2122-2130.
20. Szakal, C., S.M. Hues, J. Bennett, and G. Gillen, *The Journal of Physical Chemistry C*, 2009. **114**(12): p. 5338-5343.
21. Tanaka, K., A. Takahara, and T. Kajiyama, *Macromolecules*, 1996. **29**(9): p. 3232-3239.
22. Vickerman, J.C., *Surface Analysis: The Principal Techniques*. 2003: John Wiley & Sons Ltd.
23. Shard, A.G., S. Ray, M.P. Seah, and L. Yang, *Surface and Interface Analysis*, 2010: p. n/a-n/a.
24. Wagner, M.S., *Surface and Interface Analysis*, 2005. **37**(1): p. 62-70.
25. Wagner, M.S., *Surface and Interface Analysis*, 2005. **37**(1): p. 53-61.
26. Norrman, K., K.B. Haugshoj, and N.B. Larsen, *Journal of Physical Chemistry B*, 2002. **106**(51): p. 13114-13121.

27. Mahoney, C.M., A.J. Fahey, G. Gillen, C. Xu, and J.D. Batteas, *Applied Surface Science*, 2006. **252**(19): p. 6502-6505.
28. Lee, J.L.S., S. Ninomiya, J. Matsuo, I.S. Gilmore, M.P. Seah, and A.G. Shard, *Anal Chem*, 2010. **82**(1): p. 98-105.